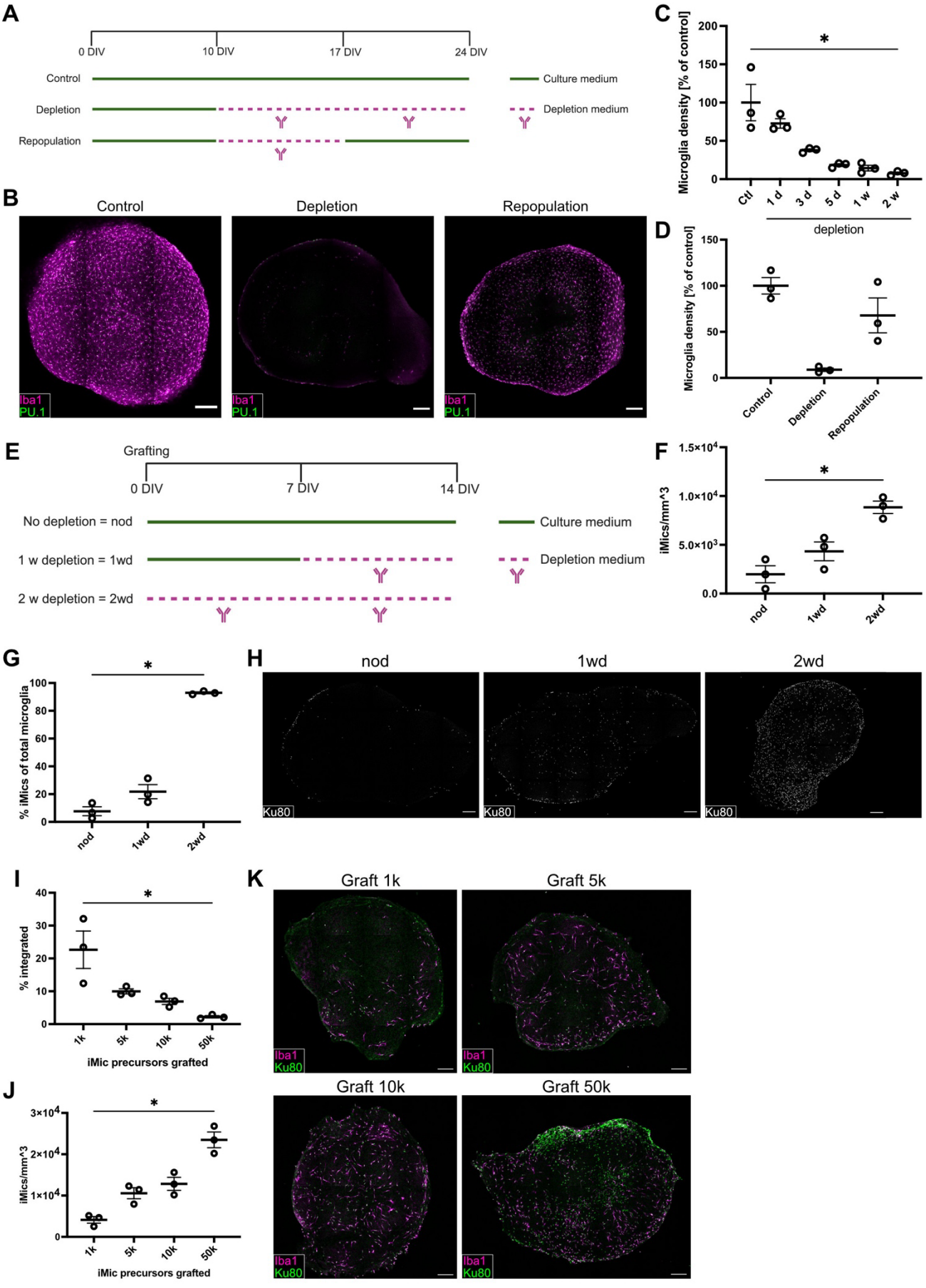

Extended Data Fig 1: **Establishment of cBSC grafting conditions**. (A) Experimental timeline of BSC. (B) Representative images of the three experimental groups from (A). After 2 weeks of depletion only 8 % of microglia were left in the

hippocampal slice cultures. After one week back in regular culture medium, microglia were beginning to repopulate the culture. Scale bars: 200 µm. (C) Microglial density in BSC with anti-CSF1R antibody as percentage of untreated BSC. n=6; number of independent experiments per group = 3; Kruskal-Wallis test with Dunn's multiple comparison test p = 0.0077. (D) Microglial density in the three experimental groups in (A). n=3; Kruskal-Wallis test with Dunn's multiple comparison test p = 0.025. (E) Experimental timeline of cBSC. (F) iMic density (number of iMics) in cBSCs in the three experimental groups in (E). n=3, Kruskal-Wallis test with Dunn's multiple comparison test p = 0.0107. (G) Grafting efficiency as percentage of iMics of total number of microglia in cBSCs. PU.1 (all myeloid nuclei) and Ku80 (human nuclei only) were used to quantify iMic engraftment in entire slices. n=3, Kruskal-Wallis test with Dunn's multiple comparison test p = 0.0036. (H) Representative images of the integration of human cells (Ku80) of the three treatment groups (as in E). Scale bars: 200 µm. (I) Percentage of iMics integrated in cBSC relative to the number grafted. n=3, Kruskal-Wallit test with Dunn's multiple comparison correction p = 0.0036. (J) iMic density at 14 DIV. n=3, Kruskal-Wallist test with Dunn's multiple comparison correction not significant (p=0.1964). (K) Representative images of 10k and 50k engraftment of iMics in cBSC at 14 DIV. Scale bar: 20 µm.

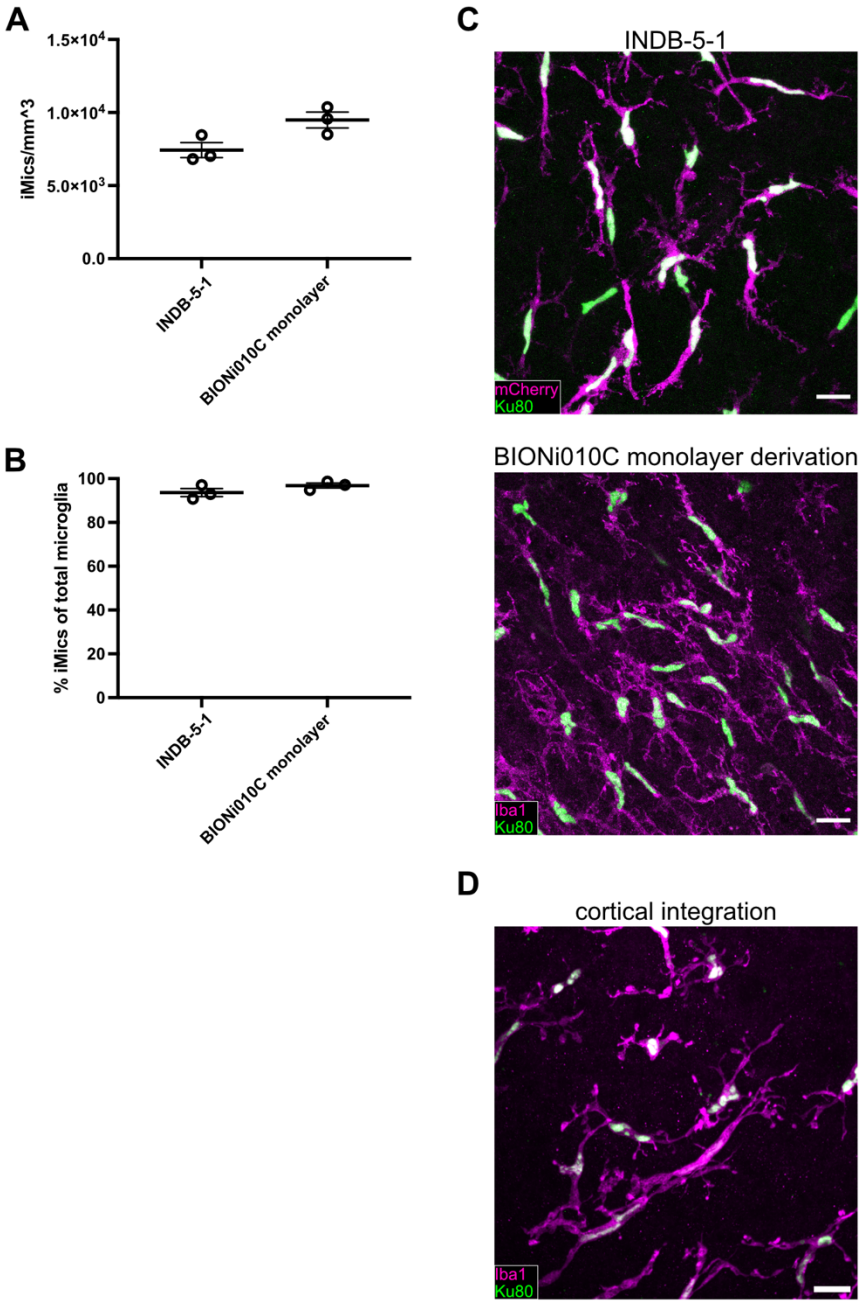

Extended Data Fig 2: **iMic integration is independent of iPSC line and microglial differentiation protocol.** (A) iMic density in cBSC. iMics were derived from two different lines (INDB-5-1, BIONi010C) and two different microglia differentiation protocols (EB-based[12] and monolayer-based[11]). (B) Grafting efficiency as the percentage of iMics (determined through Ku80 (human nuclei only)) of the total number of microglia (determined through PU.1 (all myeloid nuclei)) in the slices. (C) Representative images of iMics 14 DIV for INDB-5-1 (top, EB-based differentiation) and BIONi010C (bottom, monolayer-based differentiation) lines, respectively. (D) Representative image of iMics 21DIV in a cortical brain slice culture. Scale bars: 20 µm

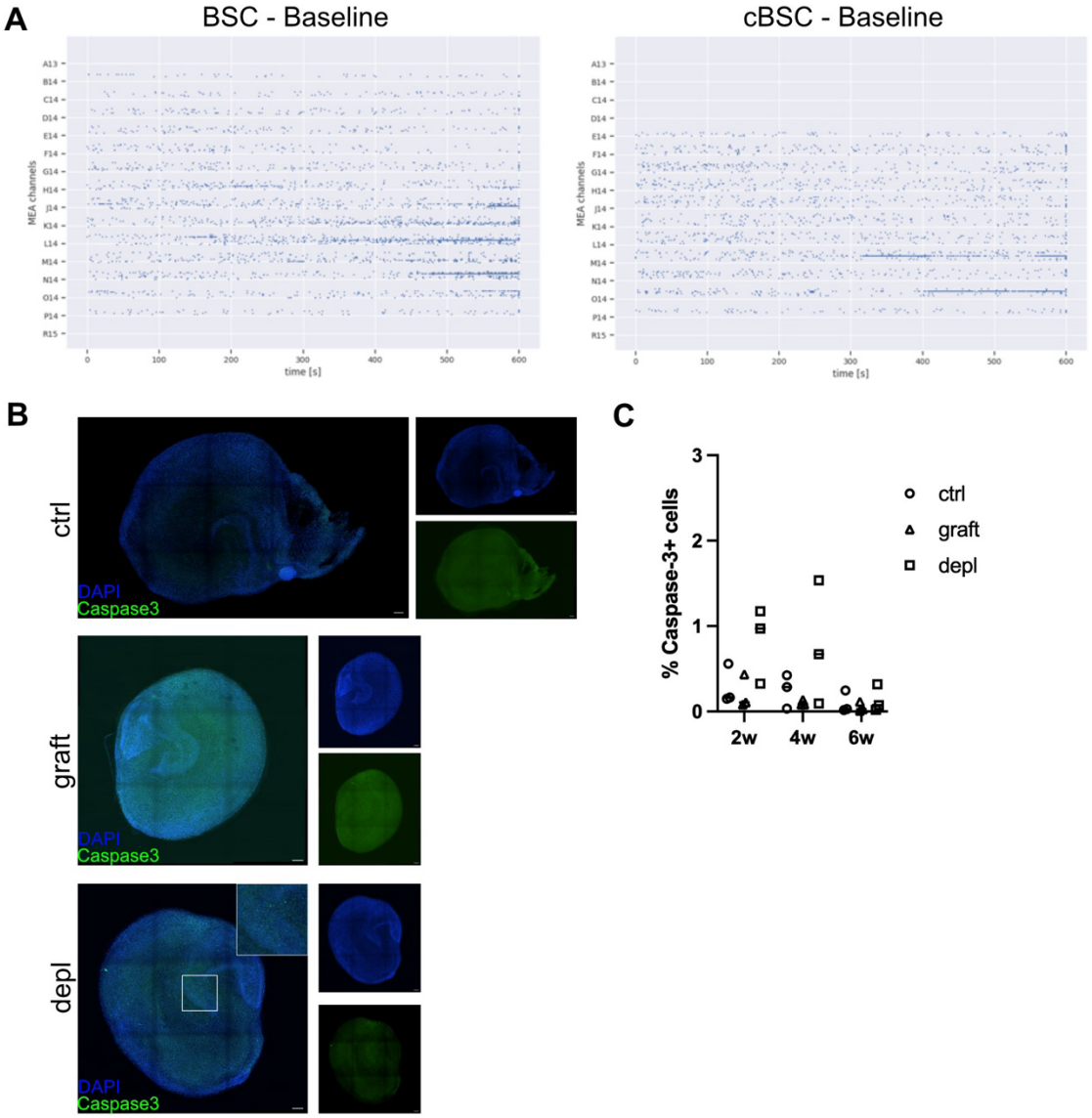

Extended Data Fig 3: **iMic engraftment does not significantly alter neuronal network activity in cBSCs.** (A) Representative spike raster plots of Micro-electrode array (MEA) recordings of spontaneous activity of BSCs and cBSCs. (B) Maximum-projection images of slices stained for nuclei (blue) and apoptotic cells (cleaved caspase 3-7, green) in control (ctrl), microglia deplete (depl), and iMic engrafted slices (graft). (C) Quantitative assessment of caspase-positive cells as a percentage of total cells (n=3).

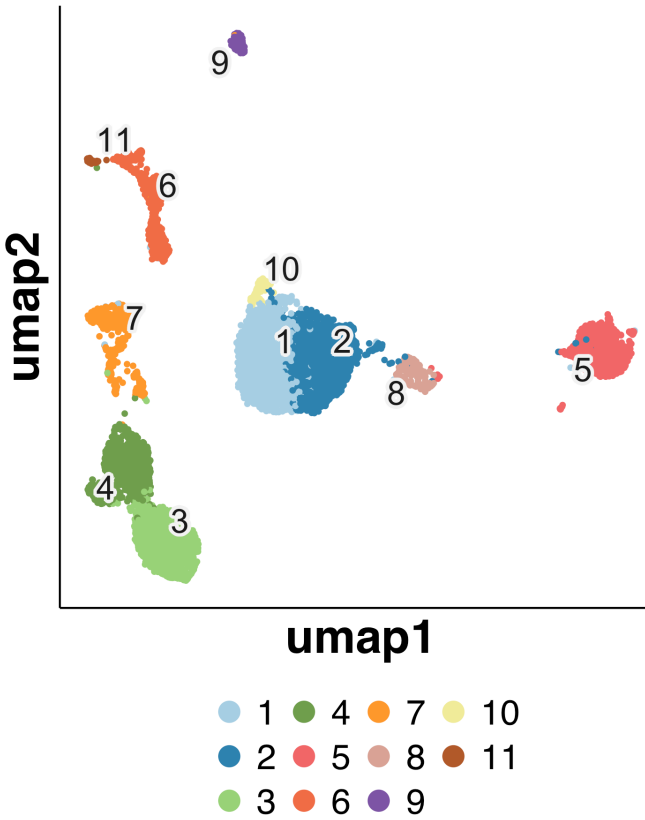

Extended Data Fig 4: **Transcriptional profile of iMics isolated from cBSCs.** Scatterplot after principal component analysis and Uniform Manifold Approximation and Projection (UMAP), colored by cluster (see Fig. 3(H)) prior to removal of neuronal and radial glial clusters 3, 4, 6, 7, 9, and 11 (*GRIA2, STMN2, MYT1L, DCX and* SOX2, *SOX9, CRYAB* respectively).

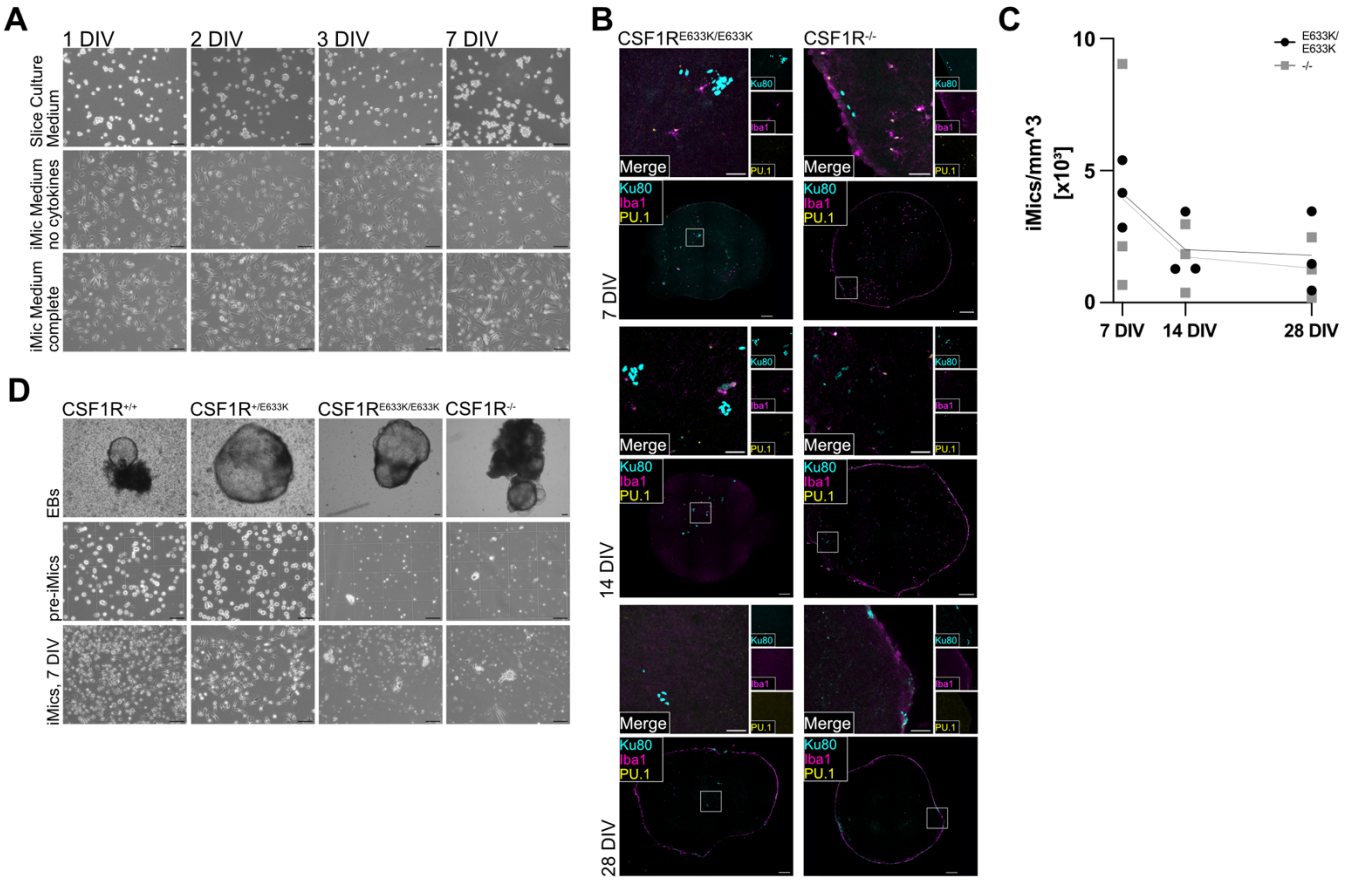

Extended data Fig 5: **CSF1R signaling is required for iMic differentiation in 2D and 3D.** (A) iMic-precursor cells plated at 20,000 cells/cm^2 in Slice Culture Medium did not adhere to the culture vessel and remained undifferentiated for 7 days. In iMic medium precursor cells attached by 1 DIV and showed ramified morphology. Scale bars: 50 µm. (B) Homozygous CSF1R mutant (E663K) or knockout (KO) iPSCs can form embryoid bodies (EB), however, pre-iMic quantities were lower and pre-iMics were smaller compared to WT or heterozygous lines. Heterozygous iMics matured in 2D similarly to WT over 7 DIV, while CSF1R$^{E633K/E633K}$ and CSF1R$^{-/-}$ differentiation was futile. Scale bars: 50 µm. (C) Also, when grafted to slice cultures, while CSF1R$^{E633K/E633K}$ and CSF1R$^{-/-}$ iMics did not differentiate, as indicated by absence of PU.1 (yellow) and Iba1 (magenta) signal for Ku80-positive nuclei (cyan). Scale bars for overview images: 200 µm, for zoom-ins: 50 µm. (D) iMic density at 7, 14 and 28 DIV. n=3 biological replicates with each dot representing the average of 3 technical replicates.

A

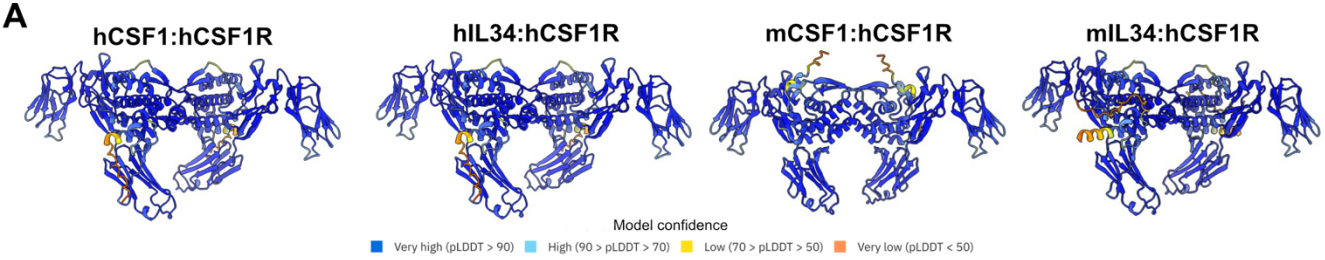

B

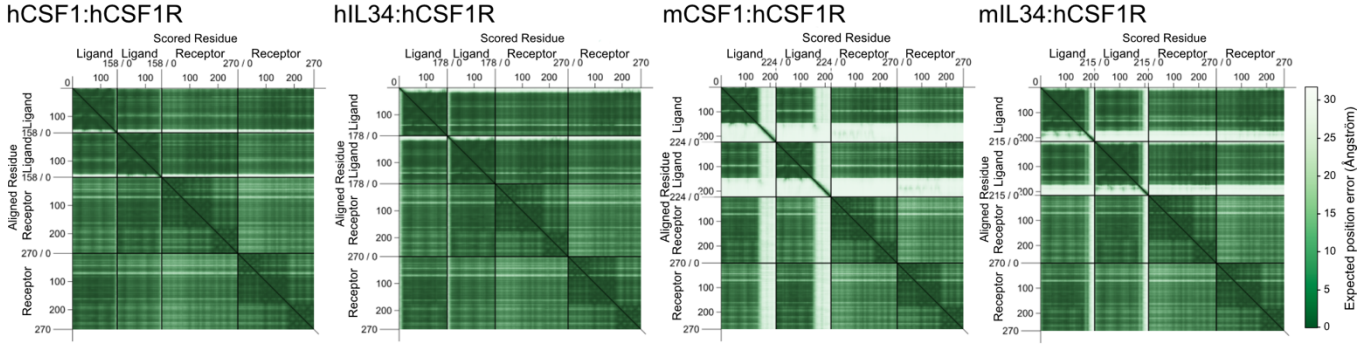

C

hCSF1:hCSF1R			
Hydrogen Bonds			
	hCSF1	hCSF1R	Dist. [Å]
1	TYR 6[HH]	ASP 234[OD2]	2.04
2	SER 13[H]	ASP 251[OD1]	2.35
3	GLY 14[H]	ASP 251[OD1]	1.81
4	GLN 79[HE22]	ASN 255[OD1]	2.11
5	GLU 62[OE2]	ARG 142[HH22]	1.71
6	ASP 59[OD2]	ARG 144[HH12]	1.86
7	ASP 59[OD1]	ARG 144[HH21]	1.83
8	ASP 63[OD2]	ARG 146[HH11]	1.67
9	ASP 63[OD1]	ARG 146[HH21]	1.83
10	GLU 62[OE2]	ARG 146[HH22]	1.83
11	ASP 69[OD2]	ARG 150[HE]	2.35
12	ASP 69[OD2]	ARG 150[HH22]	1.95
13	GLU 1[OE1]	LYS 194[HZ3]	1.78
14	GLU 82[OE1]	LYS 197[HZ3]	1.78
15	MET 10[O]	TYR 257[HH]	1.99
16			
17			
Salt Bridges			
	hCSF1	hCSF1R	Dist. [Å]
1	GLU 62[OE2]	ARG 142[NH1]	3.50
2	GLU 62[OE1]	ARG 142[NH2]	2.66
3	GLU 62[OE2]	ARG 142[NH2]	2.71
4	ASP 59[OD2]	ARG 144[NH1]	2.84
5	ASP 59[OD1]	ARG 144[NH1]	3.95
6	ASP 59[OD2]	ARG 144[NH2]	3.09
7	ASP 59[OD1]	ARG 144[NH2]	2.76
8	ASP 59[OD1]	ARG 146[NE]	3.58
9	GLU 62[OE2]	ARG 146[NE]	3.76
10	ASP 59[OD1]	ARG 146[NH1]	3.91
11	ASP 63[OD1]	ARG 146[NH1]	3.32
12	ASP 63[OD2]	ARG 146[NH1]	2.68
13	ASP 59[OD1]	ARG 146[NH2]	3.75
14	ASP 63[OD1]	ARG 146[NH2]	2.76
15	ASP 63[OD2]	ARG 146[NH2]	3.31
16	GLU 62[OE2]	ARG 146[NH2]	2.82
17	ASP 69[OD1]	ARG 150[NE]	2.94
18	ASP 69[OD2]	ARG 150[NE]	3.10
19	ASP 69[OD1]	ARG 150[NH2]	3.66
20	ASP 69[OD2]	ARG 150[NH2]	2.83
21	ASP 69[OD1]	HIS 151[NE2]	2.97
22	ASP 69[OD2]	HIS 151[NE2]	3.02
23	GLU 1[OE1]	LYS 194[NZ]	2.77
24	GLU 82[OE1]	LYS 197[NZ]	2.78
25	GLU 82[OE2]	LYS 197[NZ]	3.47

hIL34:hCSF1R			
Hydrogen Bonds			
	hIL34	hCSF1R	Dist. [Å]
1	LEU 186[H]	GLN 248[O]	2.07
2	ASN 187[HD21]	SER 250[O]	1.92
3	LYS 44[HZ1]	PHE 252[O]	1.77
4	LYS 117[HZ2]	ASN 254[OD1]	1.70
5	GLU 103[OE1]	ARG 142[HH11]	1.89
6	GLU 103[OE2]	ARG 142[HH22]	1.79
7	GLU 143[OE1]	ARG 144[HE]	1.89
8	TYR 92[OH]	ARG 144[HH22]	2.21
9	GLU 143[OE2]	ARG 144[HH21]	2.09
10	GLU 103[OE1]	ARG 146[HH22]	1.90
11	GLU 103[OE2]	ARG 146[HH21]	1.95
12	ASP 107[O]	ARG 150[HH12]	1.97
13	SER 184[O]	GLN 248[H]	2.30
14	ASN 187[OD1]	SER 250[H]	1.86
15	GLU 121[OE1]	ASN 254[H]	2.00
Salt Bridges			
	hIL34	hCSF1R	Dist. [Å]
1	GLU 103[OE1]	ARG 142[NH1]	2.88
2	GLU 103[OE2]	ARG 142[NH1]	3.85
3	GLU 103[OE1]	ARG 142[NH2]	3.24
4	GLU 103[OE2]	ARG 142[NH2]	2.76
5	GLU 143[OE2]	ARG 144[NE]	3.53
6	GLU 143[OE1]	ARG 144[NE]	2.89
7	GLU 143[OE2]	ARG 144[NH2]	3.07
8	GLU 143[OE1]	ARG 144[NH2]	3.78
9	GLU 103[OE1]	ARG 146[NH1]	3.58
10	GLU 103[OE1]	ARG 146[NH2]	2.70
11	GLU 103[OE2]	ARG 146[NH2]	2.66
12	ASP 107[OD1]	ARG 150[NH1]	3.59
13	GLU 111[OE1]	HIS 151[NE2]	3.43

mCSF1:hCSF1R			
Hydrogen Bonds			
	mCSF1	hCSF1R	Dist. [Å]
1	ASN 85[HD21]	PHE 169[O]	2.30
2	ASN 85[HD22]	ILE 170[O]	2.05
3	ASN 13[H]	ASP 251[OD1]	2.29
4	GLY 14[H]	ASP 251[OD1]	1.85
5	ASN 13[HD22]	ASP 251[OD2]	2.40
6	GLN 58[O]	ARG 146[HH11]	2.47
7	ASP 59[OD1]	ARG 144[HH22]	1.78
8	ASP 59[OD1]	ARG 146[HH12]	1.79
9	ASP 59[OD2]	ARG 144[HH12]	1.71
10	ASP 62[OD2]	ARG 142[HH12]	1.71
11	ASP 62[OD2]	ARG 142[HH21]	1.82
12	ASP 69[OD1]	ARG 150[HE]	1.97
13	ASP 69[OD2]	ARG 150[HH22]	1.76
Salt Bridges			
	mCSF1	hCSF1R	Dist. [Å]
1	ASP 59[OD1]	ARG 144[NH1]	3.68
2	ASP 59[OD1]	ARG 144[NH2]	2.72
3	ASP 59[OD1]	ARG 146[NE]	3.51
4	ASP 59[OD1]	ARG 146[NH1]	2.67
5	ASP 59[OD2]	ARG 144[NH1]	2.71
6	ASP 59[OD2]	ARG 144[NH2]	3.06
7	ASP 62[OD1]	ARG 142[NH2]	3.53
8	ASP 62[OD2]	ARG 146[NH1]	3.24
9	ASP 62[OD2]	ARG 146[NH2]	3.96
10	ASP 62[OD2]	ARG 142[NH1]	2.67
11	ASP 62[OD2]	ARG 142[NH2]	2.73
12	ASP 69[OD1]	ARG 150[NE]	2.83
13	ASP 69[OD1]	ARG 150[NH2]	3.49
14	ASP 69[OD1]	HIS 151[NE2]	2.72
15	ASP 69[OD2]	ARG 150[NE]	3.31
16	ASP 69[OD2]	ARG 10[NH2]	2.75
17	ASP 69[OD2]	HIS 151[NE2]	3.53
18	GLU 82[OE1]	LYS 197[NZ]	2.73
19	GLU 82[OE2]	LYS 197[NZ]	2.73

mIL34:hCSF1R			
Hydrogen Bonds			
	mIL34	hCSF1R	Dist. [Å]
1	ARG 131[HH22]	SER 172[OG]	2.16
2	ARG 131[HH21]	VAL 195[O]	1.95
3	LYS 187[HZ3]	SER 250[O]	1.83
4	LYS 187[HZ2]	ASP 251[OD1]	1.96
5	LYS 44[HZ2]	PHE 252[O]	1.82
6	LYS 107[HZ2]	ASN 254[OD1]	1.70
7	ASN 128[HD21]	TYR 257[OH]	1.92
8	GLU 103[OE1]	ARG 142[HH11]	2.03
9	GLU 103[OE2]	ARG 142[HH21]	1.77
10	GLU 143[OE1]	ARG 144[HE]	1.92
11	GLU 143[OE2]	ARG 144[HH21]	1.87
12	GLU 103[OE2]	ARG 146[HH22]	2.01
13	GLU 103[OE1]	ARG 146[HH21]	1.96
14	ASP 107[O]	ARG 150[HH11]	2.17
15	LEU 109[O]	ARG 150[HH21]	2.46
16	GLU 121[OE1]	ASN 254[H]	2.13
17	GLU 121[OE1]	ASN 255[H]	2.13
Salt Bridges			
	mIL34	hCSF1R	Dist. [Å]
1	LYS 187[NZ]	ASP 251[OD1]	2.88
2	GLU 103[OE2]	ARG 142[NH1]	3.73
3	GLU 103[OE1]	ARG 142[NH1]	3.03
4	GLU 103[OE2]	ARG 142[NH2]	2.76
5	GLU 103[OE1]	ARG 142[NH2]	3.52
6	GLU 143[OE1]	ARG 144[NE]	2.89
7	GLU 143[OE2]	ARG 144[NE]	3.15
8	GLU 143[OE1]	ARG 144[NH2]	3.95
9	GLU 143[OE2]	ARG 144[NH2]	2.83
10	GLU 103[OE1]	ARG 146[NH1]	3.90
11	GLU 103[OE2]	ARG 146[NH2]	2.70
12	GLU 103[OE1]	ARG 146[NH2]	2.78

Extended data Fig 6: **Alphafold 2 prediciton of the ternary complexes of hCSF1R with its cognate human or respective murine ligands.** (A) The alphafold2 model of the ternary complex of two hCSF1R$_{D1-D3}$ molecule with its cognate dimerized ligand human CSF1 or IL34, or the dimerized murine counterpart mCSF1 or mIL34. The prediction

is colour-coded by the pLDDT values indicating the confidence level of the prediction. Dark blue – very high confidence (pLDDT > 90), light blue – confident (90 > pLDDT > 70), yellow – low (70 > pLDDT > 50), orange – very low (pLDDT <50). (B) Predicted aligned error of the predicted ternary complexes. (C) Predicted interactions at the hCSF1R$_{D1-D3}$:ligand interface in the alphafold2 model predictions.

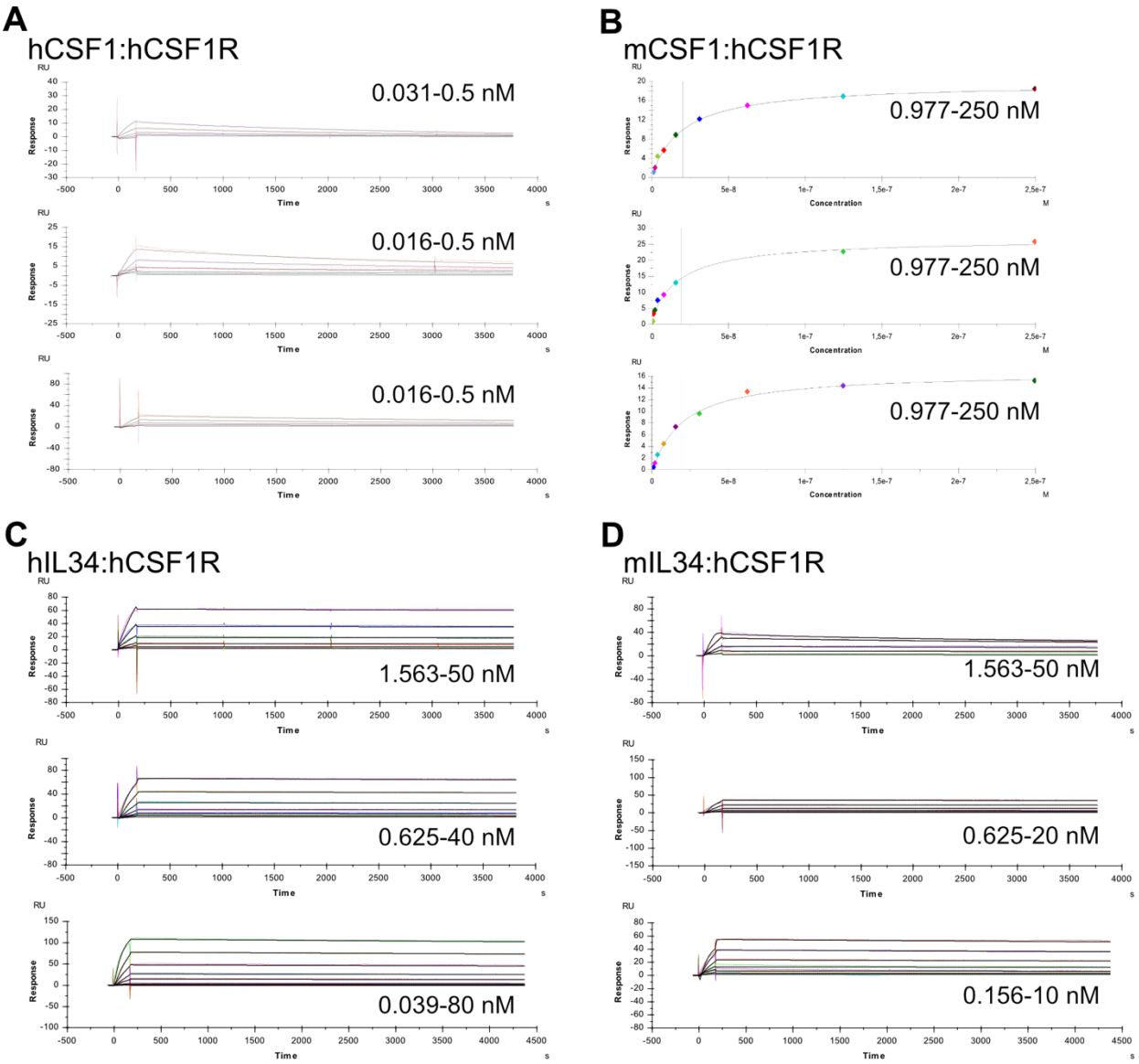
A
hCSF1:hCSF1R
0.031-0.5 nM
0.016-0.5 nM
0.016-0.5 nM
B
mCSF1:hCSF1R
0.977-250 nM
0.977-250 nM
0.977-250 nM
C
hIL34:hCSF1R
1.563-50 nM
0.625-40 nM
0.039-80 nM
D
mIL34:hCSF1R
1.563-50 nM
0.625-20 nM
0.156-10 nM
RU
Response
Time
Concentration
M
s

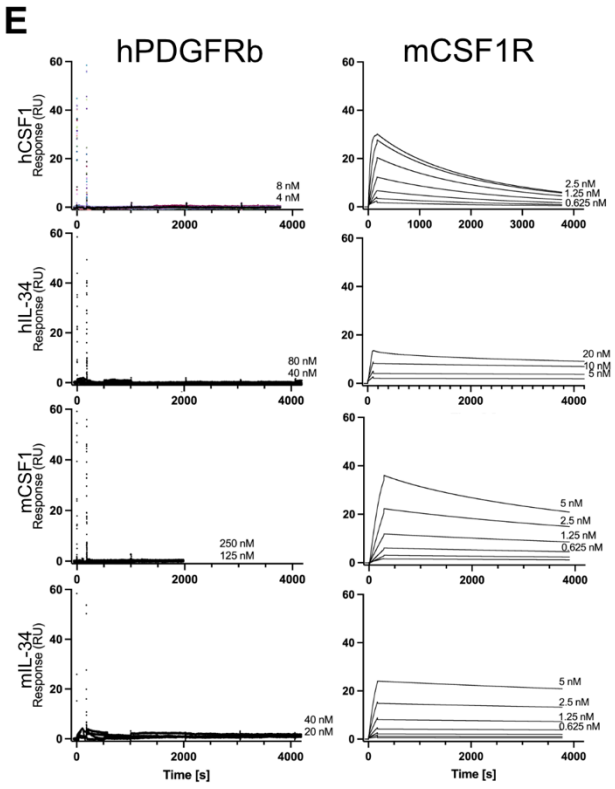
E
hPDGFRb
mCSF1R
hCSF1
hIL-34
mCSF1
mIL-34
Response (RU)
8 nM
4 nM
2.5 nM
1.25 nM
0.625 nM
80 nM
40 nM
20 nM
10 nM
5 nM
250 nM
125 nM
5 nM
2.5 nM
1.25 nM
0.625 nM
40 nM
20 nM
5 nM
2.5 nM
1.25 nM
0.625 nM
Time [s]

59
60

Extended data Fig 7: **Ligand binding to CSF1R as assessed by surface plasma resonance**. Kinetic binding parameters were determined by Biacore-SPR. (A-D) Sensogram plots generated by SPR kinetic analysis demonstrate the association and dissociation characteristics between immobilized ligand (hCSF1R) and analytes (hCSF1, mCSF1, hIL34, and mIL34). (E) PDGFRb, like CSF1R a member of the receptor tyrosine kinase type II subfamily, was used as a negative control.

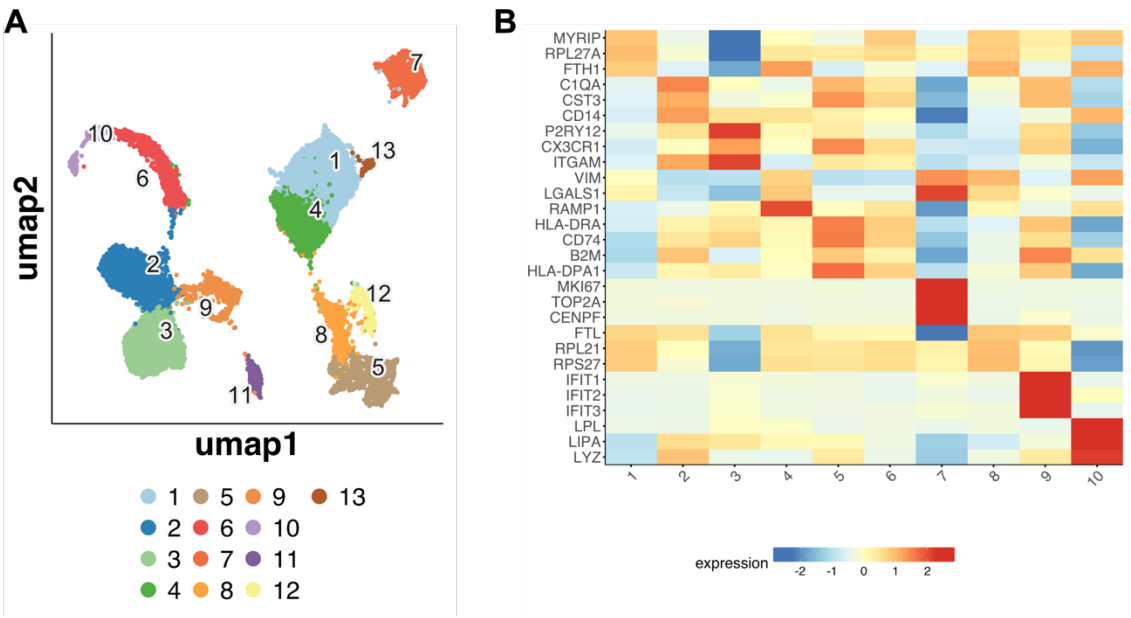

Extended Data Fig 8: **Transcriptional profile of iMics isolated from cBSCs with and without aSyn pathology.** (A) Scatterplot after principal component analysis and Uniform Manifold Approximation and Projection (UMAP), colored by cluster prior to removal of neuronal and radial glial clusters 2, 3, 5, 6, 8, 9, 10, and 11 (*GRIA2, STMN2, MYT1L, DCX and* SOX2, *SOX9, CRYAB* respectively). (B) Heatmap for differentially expressed genes of clusters 1-10 of Fig. 5E.